PII: S0032-3861(97)00450-3

Determination of parameters in mechanical model for cellulose III fibre

Atsuko Ishikawa†‡*, Shigenori Kuga and Takeshi Okano
The University of Tokyo, Graduate School of Agricultural and Life Sciences, Bunkyo-ku, Tokyo 113, Japan

Tensile properties and fine structure of ramie cellulose III_I obtained with either ethylenediamine or liquid ammonia were compared. The fibre treated with ethylenediamine had lower crystallinity index, elastic modulus and tensile strength, and greater internal surface area and strain-at-break than the fibre treated with liquid ammonia. The load–elongation behaviour of the fibres was interpreted by using a two-phase parallel–series mechanical model comprising two types of springs representing the crystalline and amorphous components to give a single value of the elastic constant for the cellulose III crystal. The analysis gave sets of model parameters, revealing a remarkable difference in the mechanical contribution of crystal and amorphous components in the two samples. Calculation based on these results gave an elastic modulus of 115–122 GPa for the cellulose III crystallite, and 4.6–8.2 and 9.6–10 GPa for the amorphous components in ethylenediamine and liquid ammonia-treated fibres, respectively. © 1998 Elsevier Science Ltd. All rights reserved.

(Keywords: ramie cellulose; cellulose III; mechanical model)

INTRODUCTION

Treatment of native cellulose fibre with liquid ammonia and amines has been of interest from both academic and industrial viewpoints. Treatment of cellulose I with these agents results in full or partial conversion of cellulose I into cellulose III_I, depending on the treating conditions and the way of removing the agent. Extensive work has been done on the mechanism of this conversion process[1–5]. In the meantime, Gogek et al.[6] and Calamari et al.[7] separately reported that pretreatment of cotton with liquid ammonia improved abrasion resistance, resiliency, tensile properties and wrinkle resistance of subsequently cross-linked fabric. Rousselle et al.[8] reported that slack treatment with liquid ammonia gave an increase in the elongation-at-break, while treatment under tension gave an increase in tenacity. The mechanism of such changes in the mechanical properties, however, has not been well understood at the molecular and fine structure levels.

Since the cellulose fibre, both natural and regenerated, is composed of crystalline and amorphous regions, it is important to understand the nature of these components and their contributions to the macroscopic mechanical properties of the fibre. By giving a fibre tensile strain and measuring the resulting stress and change in X-ray diffraction, one can determine the elastic modulus of the fibre and the strain of the crystallites; however, there is no method to directly determine the actual stress (tensile force) exerted to the crystallites.

In the previous study, we proposed a mechanical model to qualitatively explain the relation between macroscopic and

crystal strains of fibres composed of four types of cellulose crystals (cellulose I (original), cellulose II, cellulose III_I, cellulose IV_I) prepared from ramie[9]. With a single sample for each crystal form, however, it was not possible to determine the composition and elastic moduli of the crystal and amorphous components.

In this study, we examined two types of cellulose III_I fibre samples prepared from ramie by liquid ammonia and ethylenediamine treatments, intending to determine the above-mentioned parameters from a comparison between two samples with different fine structures but containing the same type of crystallites. Namely, a comparison of crystal lattice strain under tensile stress should give quantitative information on the structure of the amorphous region, which transfers the load to the crystallites.

EXPERIMENTAL

Sample preparation

Two types of cellulose III_I fibre samples were prepared as follows:

(1) Ethylenediamine treatment. Purified native ramie fibres (cellulose I) supplied by Teikoku Bouseki Co., Ltd. (Tokyo) were soaked in 75% ethylenediamine for 1 h and rinsed with methanol[5]. This procedure was repeated five times until the fibre yielded the typical X-ray diagram of cellulose III_I.

(2) Liquid ammonia treatment. The native ramie fibre was immersed in liquid ammonia at $-33°C$ in a stainless steel pressure vessel. The mixture was allowed to stand at room temperature for 2 days and then heated to 140°C (over the critical temperature of ammonia, 132.5°C) for 1 h. Ammonia was removed at this temperature by venting the vessel.

Both samples showed typical X-ray equatorial diffraction

* To whom correspondence should be addressed
† Present address: Forestry and Forest Products Research Institute, PO Box 16, Tsukuba Norin Kenkyu Danchi-Nai, Ibaraki 305, Japan
‡ Tel.: + 81-298-73-3211 ext. 579; fax: + 81-298-73-3798;
e-mail: aishi@ffpri.affrc.go.jp

patterns of cellulose III₁ (*Figure 1*). Hereafter these samples are referred to as cellulose III (EDA) and cellulose III (NH₃), respectively.

The density of the cellulose sample was determined by a pycnometer using xylene and carbon tetrachloride as reference liquids. The densities were 1.488 and 1.483 g/cm³ for cellulose III (EDA) and cellulose III (NH₃), respectively.

X-ray diffractometry

X-ray diffraction and crystal strain measurements were performed by using bundles of 100 ramie fibres as shown in *Figure 2*. X-ray diffraction measurements were made by the transmission method. Ni-filtered Cu Kα radiation ($\lambda = 0.1542$ nm) generated at 40 kV and 80 mA by a Rigaku RU-200BH generator was collimated through a pinhole of 2 mm ϕ with a length of 75 mm. The diffraction intensity was recorded by a goniometer equipped with a scintillation counter at a scanning speed of 0.5°/min and sampling rate of 1 point/s. The measurement was made separately for meridional and equatorial diffractions of the fibre sample.

For each diffraction pattern, the crystal diffraction components were separated from scattering from the amorphous regions. For both meridional and equatorial

diffraction patterns, the amorphous scattering was represented by two broad Gaussian peaks[10]. The integral crystallinity index was determined from the ratio of the sum of integrated intensities of 1$\bar{1}$0, 110 and 200 reflections (fibre axis is c) to the total equatorial diffraction intensity in the range of 2θ from 10 to 25°. The average crystallite width and length were calculated from 1$\bar{1}$0 and 110, and 004 peak widths, respectively, based on Scherrer's equation[11] corrected by NaF reflection.

The crystal strain measurement was made by applying a tensile strain to the bundle specimen by a manually driven straining frame equipped with a strain gauge. The sample assembly was mounted on the diffractometer and the macroscopic tensile load and diffraction pattern were recorded simultaneously.

The crystal lattice strain (ε_c) in the longitudinal direction was determined from the increase in 004 spacing induced by the tensile force, according to the following equation obtained by differentiating Bragg's equation:

$$\varepsilon_c = \frac{\Delta d}{d} = -\Delta\theta \cot \theta \qquad (1)$$

where d is the lattice spacing.

Elastic modulus, breaking strength and strain-at-break

The mechanical properties of native and converted ramie fibres were determined by single-fibre measurements. Both ends of a single fibre were clamped, with a span of 11 mm, by a pair of cardboard pieces with epoxy resin in a similar way to that shown in *Figure 2*. Tensile tests were performed on a Tensilon UTM-III-100 (Toyo Baldwin Co., Tokyo) at 65% RH, 20°C with a tensile speed of 10 mm/min. The cross-sectional area of the specimen was determined from a cross-sectional SEM image of the same specimen used for the tensile test. The result was obtained as an average of more than 50 runs of measurements for each sample.

Internal surface area

The water adsorption isotherm of the fibre was obtained by weighing the sample equilibrated at various relative humidities by LiCl and saturated solutions of MgCl₂ and K₂CO₃. The internal surface area was calculated from the isotherm according to the Brunauer–Emmett–Teller (BET) theory[12].

Figure 1 Equatorial diffraction curves of ramie fibers: (a) original, treated with (b) ethylenediamine, and (c) liquid NH₃

Figure 2 Specimen for X-ray diffraction

RESULTS AND DISCUSSION

Fine structure and crystallite size

Table 1 shows the integral crystallinity index, internal surface area and crystallite size of original (cellulose I), ethylenediamine-treated (cellulose III (EDA)), and liquid ammonia-treated (cellulose III (NH₃)) ramie fibres. While the integral crystallinity index of cellulose III (EDA) was reduced significantly (59% of the original value), that of cellulose III (NH₃) was slightly increased (105%). On the other hand, the crystallite width determined by Scherrer's
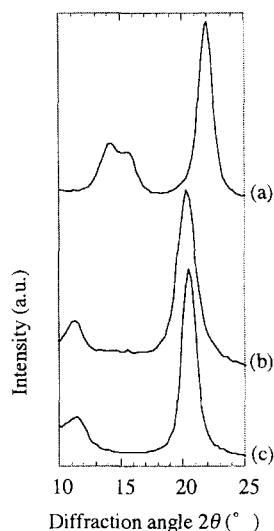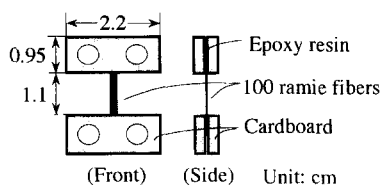
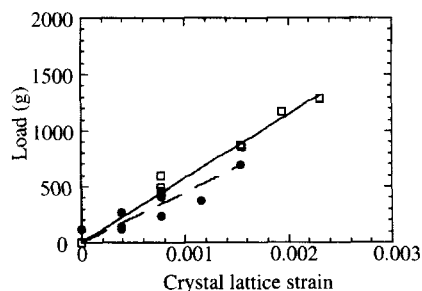**Table 1** Properties of ramie cellulose I and ramie cellullose III₁ obtained with ethylenediamine and liquid NH₃

	Crystallinity index (%)	Crystallite width (nm)	Crystallite length (nm)	Internal suface area (m²/g)
Cellulose I	64 (100)[a]	4.8 (100)	18.7 (100)	133 (100)
Cellulose III₁ (EDA)	38 (59)	5.1 (106)	15.0 (80)	172 (129)
Cellulose III₁ (liq. NH₃)	67 (105)	7.4 (154)	14.2 (76)	164 (123)

[a]Percentage of the values to the value for cellulose I

Table 2 Tensile properties of ramie cellulose I and ramie cellulose III$_1$ obtained with ethylenediamine and liquid NH$_3$

	E_f (GPa)	σ_b (MPa)	ε_b ($\times$ 10^{-2})
Cellulose I	27 (100)[a]	755 (100)	3.2 (100)
Cellulose III$_1$ (EDA)	15 (56)	693 (92)	5.8 (181)
Cellulose III$_1$ (liq. NH$_3$)	46 (170)	702 (93)	2.8 (88)

E_f = elastic modulus of fiber; σ_b = tensile strength; ε_b = strain-at-break
[a] Percentage of the values to the value for cellulose I

Figure 3 Relationship between load and crystal lattice strain of ramie cellulose III obtained with ethylenediamine and liquid NH$_3$, respectively: – □ –, cellulose III (EDA); – • –, cellulose III (liq. NH$_3$)

Figure 4 Parallel–series model: A, amorphous component; C, crystalline component

equation was increased to 106 and 154% of the original width by EDA and liq. NH$_3$ treatments, respectively; the crystallite length, in contrast, was decreased to 80 and 76%, respectively.

These changes indicate that the cellulose I crystallites in the original ramie fibre were converted to cellulose III$_1$ crystallites with a strong dependence of the resulting morphology on the type of converting agent. The remarkable increase (from 133 to 164 m^2/g) in the surface area by liq. NH$_3$ treatment is not consistent with the moderate increase (from 64 to 67%) in the crystallinity index. This behaviour must be interpreted as showing a significant modification in the structure of the amorphous regions induced by the conversion. The difference in the molecular size and the way of removing the agent might cause such variations in the fine structure[4,5].

Tensile properties

The tensile properties of the samples are shown in *Table 2*. The elastic modulus of the fibre (E_f) was reduced to 56% of the original value by EDA treatment, but significantly increased (to 170%) by liq. NH$_3$ treatment. Both agents slightly lowered the tensile strength (σ_b), while the strain-at-break (ε_b) decreased with liq. NH$_3$ to 88% and increased to 181% with EDA. These features, together with those of the X-ray diffraction measurements stated above, indicate that EDA treatment causes reduction in the crystalline

nature and softening of the ramie fibre, whereas liq. NH$_3$ treatment results in enhancement of crystallinity and stiffening of the fibre.

Two-phase model interpretation of elastic modulus

The crystal lattice strain (ε_c) of cellulose III (EDA) was smaller than that of cellulose III (NH$_3$) at the same load as shown in *Figure 3*. Because the crystallites in these samples have the same structure of cellulose III$_1$, there must be a difference between the two samples in the manner by which the amorphous region transfers the macroscopic tensile force to the crystallites.

We consider a parallel–series model consisting of one crystal component and two amorphous components shown in *Figure 4*[9]. By defining the longitudinal and lateral fractions of the individual components, m and n, as indicated in the figure, the elastic moduli of the crystal component (E_c) and the amorphous component (E_a) are given as follows using the modulus of the fibre (E_f):

$$\frac{E_c}{E_f} = \frac{1}{n}\left\{ \frac{1}{k} - \frac{(1-m)(1-n)}{1-km} \right\} \qquad (2)$$

$$\frac{E_a}{E_f} = \frac{1-m}{1-km} \qquad (3)$$

where $k = \varepsilon_c/\varepsilon_f$ and ε_f is the strain of the fibre. On the other hand, the following relations hold between the densities of the fibre (ρ_f), the crystal component (ρ_c), and the amorphous component (ρ_a), and the integral crystallinity index (CrI):

$$\rho_f = mn\rho_c + (1 - mn)\rho_a \qquad (4)$$

$$\rho_f CrI = mn\rho_c \qquad (5)$$

From equations (4) and (5) we obtain

$$\rho_a = \frac{\rho_c\rho_f(1 - CrI)}{\rho_c - \rho_f CrI} \qquad (6)$$

By using experimental values for ρ_f, CrI, and ρ_c (from lattice constants[13]), ρ_a is calculated to be 1.45 and 1.34 g/cm^3 for cellulose III (EDA) and cellulose (NH$_3$), respectively.

Our goal is to determine the elastic moduli of the crystal component (E_c) and the amorphous component (E_a) and values of m and n by using these relations. These quantities can have different values for the two cellulose III samples. From equations (2), and (5) we obtain

$$E_c = \frac{E_f}{n}\left\{ \frac{1}{k} - (1-n)\frac{n\cdot\rho_c - \rho_f\cdot CrI}{n\cdot\rho_c - \rho_f\cdot CrI\cdot k} \right\} \qquad (7)$$

which can be plotted against n for the two samples as in *Figure 5*. The basic assumption is that the crystal components in these samples have the same value of the elastic modulus E_c. The horizontal broken lines in *Figure 5* show the range of E_c values that satisfies this requirement. Thus we obtain E_c of 115–122 GPa (common) and n of 0.67–0.7 for cellulose III (NH$_3$) and 0.94–1 for cellulose III (EDA). This value of E_c is significantly greater than the previously reported value of 87 GPa for cellulose III (NH$_3$) (Nishino *et al.*[14]). While the latter value was obtained by assuming a series model, the present result is based on a parallel–series model and is likely to be closer to the
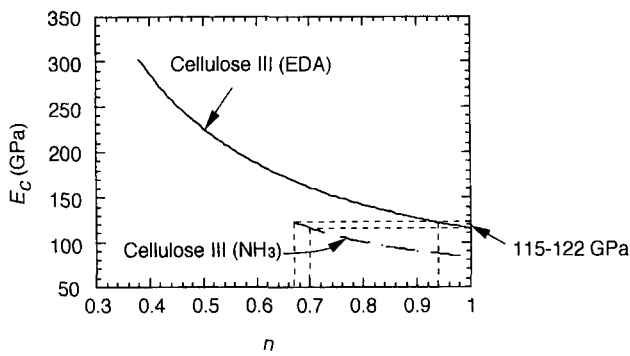
Figure 5 Relationship between the elastic modulus of the crystalline component (E_c) and the width of the crystalline component (n) in the parallel–series model shown in *Figure 4*: ——, cellulose III (EDA); — – —, cellulose III (NH_3)
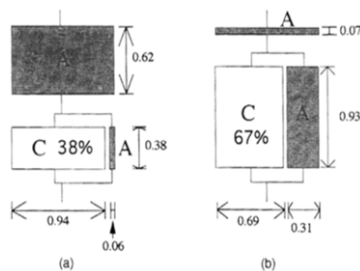

Figure 6 Parallel–series mechanical model for ramie fiber treated with (a) ethylenediamine and (b) liquid NH_3
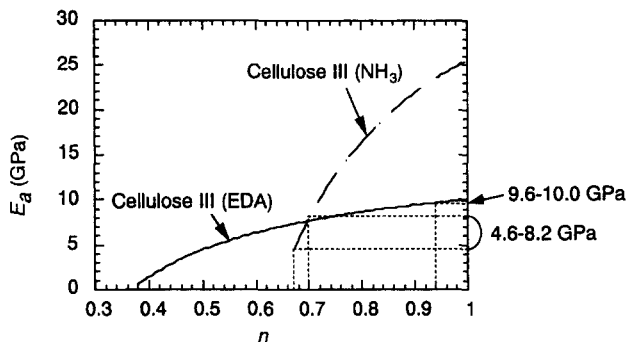

Figure 7 Relationship between the elastic modulus of the amorphous component (E_a) and the width of the crystalline component (n) in the parallel–series model shown in *Figure 4*: ——, cellulose III (EDA); — – —, cellulose III (NH_3)

true value, because our model in *Figure 6* suggests that the cellulose III (NH_3) sample shows basically parallel-combination behaviour.

From these results, mechanical models for the two cellulose III samples can be represented as in *Figure 6*. There can be seen a remarkable difference between the models in the contribution of the crystalline and amorphous components. The amorphous component of cellulose III (EDA) lies mostly in series with the crystalline component, thus contributing to a low elastic modulus; on the other hand, that of cellulose III (NH_3) is mostly in parallel to the crystalline component, contributing to the stiffening of the fibre.

Having determined the values of n, we can now assess the elastic moduli of the amorphous components in the two

samples. Combining equations (3) and (5) we obtain

$$E_a = \frac{n \cdot \rho_c - \rho_f \cdot CrI}{n \cdot \rho_c - \rho_f \cdot CrI \cdot k} E_f \qquad (8)$$

With experimentally determined values of ρ_c, ρ_f, CrI, k, and E_f, equation (8) represents two E_a versus n plots for the two cellulose III samples as in *Figure 7*. The ranges of n determined in *Figure 5* can be used here to determine the possible ranges of E_a: 9.6–10.0 GPa for cellulose III (EDA) and 4.6–8.2 GPa for cellulose III (NH_3). These values are about one-tenth of E_c determined above. It is also of the same order of the experimentally measured elastic modulus of amorphous cellulose (*ca.* 8 GPa) reported by Yano and Hatakeyama[15].

CONCLUSIONS

Load–elongation behaviour of cellulose III (EDA) and cellulose III (NH_3) was interpreted by using a two-phase parallel–series mechanical model. Assuming that the crystal components in the samples have the same value of the elastic modulus, we could determine the elastic moduli and the composition of the crystal and amorphous components. These values could not be determined with a single sample for one crystalline form. The elastic modulus determined with our model is likely to be closer to the true value than that obtained with the commonly used series model, because our model incorporates both parallel and series components for the mechanical behaviour. Cellulose III (EDA) tends to show series-combination behaviour while cellulose III (NH_3) shows basically parallel-combination behaviour. The mechanical model for cellulose (NH_3) will be useful for understanding the mechanism of liquid ammonia treatment of textiles. By utilizing this method, the elastic moduli of the crystal and amorphous components and parameters for the model can be determined for other crystalline forms, if different samples are available that consist of the same type of crystallites.

REFERENCES

1. Lewin, M. and Roldan, L. G., *J. Polym. Sci., Part C*, 1971, **36**, 213.
2. Jung, H. Z., Benerito, R. R., Berni, R. J. and Mitcham, D., *J. Appl. Polym. Sci.*, 1977, **21**, 1981.
3. Saffan, A. A., Kandil, S. H. and Habib, A. M., *Text. Res. J.*, 1984, **54**, 863.
4. Yatsu, L. Y., Calamari, T. A. Jr. and Benerito, R. R., *Text. Res. J.*, 1986, **56**, 419.
5. Lokhande, H. T., Shukla, S. R., Chidambareswaran, P. K. and Patil, N. B., *J. Polym. Sci., Polym. Lett. Ed.*, 1977, **15**, 97.
6. Gogek, C. J., Olds, W. F., Valko, E. I. and Shanley, E. S., *Text. Res. J.*, 1969, **39**, 543.
7. Calamari, T. A. Jr., Schreiber, S. P., Cooper, A. S. Jr. and Reeves, W. A., *Text. Chem. Color.*, 1971, **3**, 234–261.
8. Rousselle, M. A., Nelson, M. L., Hassenboehler, C. B. Jr. and Legendre, D. C., *Text. Res. J.*, 1976, **46**, 304.
9. Ishikawa, A., Okano, T. and Sugiyama, J., *Polymer*, 1997, **38**, 463.
10. Okano, T. and Koyanagi, A., *Biopolymers*, 1986, **25**, 851.
11. Alexander, L. E., in *X-ray Diffraction Methods in Polymer Science*, Wiley, 1969, p. 423.
12. Brunauer, S., Emmett, P. H. and Teller, E., *J. Am. Chem. Soc.*, 1938, **60**, 309.
13. Sarko, A., Southwick, J. and Hayashi, J., *Macromolecules*, 1976, **9**, 857.
14. Nishino, T., Takano, K. and Nakamae, K., *J. Polym. Sci., Polym. Phys. Ed.*, 1995, **33**, 1647.
15. Yano, S. and Hatakeyama, H., *J. Appl. Polym. Sci.*, 1976, **20**, 3221.